CHAPTER II
BACKGROUND AND LITERATURE SURVEY

2.1 Principle of Deposition

Solid deposition has frequently encountered in all facets of chemical processes. The deposition of crystals on heat exchanger surfaces is common in aqueous systems. When the cold surface of a heat exchanger is exposed to warm, moist air, a layer of frost deposits, resulting in a decrease in the efficiency of the heat exchanger. In petroleum production and processing, deposition of organic material (e.g. paraffin wax) in the flow lines reduces the flow efficiency.

The solubility limit for a given condition, particularly temperature, is the cause for almost all examples of deposition discussed above. The solubility of a solute is temperature-dependent and in most cases, it increases with increasing temperature, hence if a saturated solution of a salt is cooled, salt crystals separate out from the solution. When such a solid precipitate deposits on the surface, it traps a significant amount of solvent in the interstices of the crystals. The mechanism of the deposition process on a heat exchanger tube wall can be described by the following steps (Bott, 1997).

1) Initial precipitation on the cold surface, resulting in a radial concentration gradient

2) Radial diffusion of a salt towards the interface from the bulk

3) Internal diffusion inside the deposit through the trapped solvent

4) Desolvation of the salt in the deposit

5) Radial counter-diffusion of the trapped solvent away from the surface

Steps 3) to 5) lead to hardening of the deposit, i.e., increase of the solid content of deposit.

The mechanism of frost deposition on a cold surface exposed to warm air can also be described by the above five steps. Frost deposition starts with the formation of ice columns of varying diameters and orientations. The air in contact with these sparsely distributed ice columns is stagnant and is analogous to the trapped solvent described above. These ice columns grow as more water vapor diffuses through the stagnant air and crystallizes, leading to an internal densification of frost layer (Tao *et al.*, 1993).

2.2 Wax Deposition

Wax deposition in cold flow lines is another important deposition process. When a waxy oil is cooled, it gels due to the formation of a network of wax crystals. Unlike in the case of the above-mentioned inorganic solutions, where there is hardly any interaction among salt crystals, these wax crystals have a strong interaction and affinity resulting in the formation of the network. Although oil (solvent) and wax (solute) have a similar chemical nature, their molecular weights are different. Waxes have a higher molecular weight and they tend to form stable wax crystals that interlock to form a solid network (Wardhaugh and Boger, 1991). The network of wax crystals interacts with the oil molecules and traps a large quantity of oil (Holder and Winkler, 1965). Hence, the initial stage of the deposition of the waxy oil mixture on a cold surface is the formation of a gel layer with a large fraction of trapped oil.

Waxy oil is a mixture of hydrocarbons of varying carbon numbers. When this mixture is cooled to a certain temperature, a fraction of hydrocarbons with carbon numbers above a certain value (the *critical carbon number*) precipitate out as stable crystals to form a gel, with the remaining hydrocarbons trapped in the gel network. The formation of such gels on a

cold surface is the first step of the deposition process. The trapped liquid acts as a medium for further diffusion of the heavier molecules into the gel. This diffusion of heavier molecules is accompanied by the counter-diffusion of the trapped oil (lighter hydrocarbons) out of the deposit. This process leads to an increase in the fraction of molecules with carbon number greater than the critical carbon number and a decrease in the fraction of molecules with carbon number lower than the critical carbon number, in the gel deposit. The wax deposition process can be described by the following steps:

1) Gelation of the waxy oil (i.e. formation of incipient gel layer) on the cold surface

2) Diffusion of waxes (hydrocarbons with carbon number greater than the critical carbon number) towards the gel layer from the bulk

3) Internal diffusion of these molecules through the trapped oil

4) Precipitation of these molecules in the deposit

5) Counter-diffusion of de-waxed oil (hydrocarbons with carbon number lower than the critical carbon number) out of the gel layer

Steps 3) to 5) lead to hardening of the deposit, i.e., increase of the solid wax content of the deposit. (Singh *et al.*, 1999b)

The critical carbon number would be different for different waxy oils and is also a function of the operating conditions, such as wall temperature. The higher critical carbon number makes the deposit harder resulting in more difficult of the wax removal process.

In order to select the proper technique to remove the deposit in the pipeline, the critical carbon number must be identified along with other properties of wax deposit (e.g. hardness, melting point, and heat of fusion). Thus, prediction of the critical carbon number of the wax deposits is essential.

2.3 Physics of Gel Deposition

2.3.1 Formation of the Gel Deposit

When a warm wax-oil mixture comes in contact with a cold surface, a layer of the sample near the surface loses heat and temperature of the layer goes below the cloud point of the mixture. This decrease in the temperature causes the layer to form a gel at the cold surface. This gel is a complex network of wax crystals having a large volume fraction of oil trapped into it. Temperatures of oil pipeline walls in sub-sea environment are usually below the cloud point of crude oils flowing in them. Hence, a layer of the crude oil flowing near the wall of the pipeline forms a gel. The gel layer keeps on growing until the pipe is partially plugged. (Singh *et al.*, 1999a)

2.3.2 Aging Mechanisms of the Gel Deposit

The wax content of the gel deposit increases with time and this aging process leads to hardening of the deposit. The temperature gradient across the deposit and the mechanical force due to the flow are expected to be responsible for the aging of the gel deposit. The thermal gradient (therefore, the concentration gradient) across the deposit may cause diffusion of the wax molecules into the deposit. The mechanical force on the gel deposit exerted by the flow of the fluid over the deposited layer may squeeze the oil out of the gel deposit, which leads to an increase in the wax content of the deposit with time, i.e. harden the gel deposit. (Singh *et al.*, 1999b)

2.3.2.1 Thermal Gradient

The solubility of the wax in the oil solvent is a strong function of temperature. Therefore, the radial thermal gradient in the pipeline causes a radial concentration gradient of wax as well as oil. The concentration of wax at the wall of the pipeline is low because of the low wall temperature as compared to that in the bulk. This concentration gradient leads to the radial

diffusion of wax towards the wall of the pipeline. Similarly, the oil diffuses away from the wall due to the concentration gradient of oil. This process is a counter diffusion of the wax and the oil. The incipient gel deposit is a 3D matrix of wax crystals having nearly 90-95% oil trapped in it. Hence, wax molecules continue to diffuse into the gel layer and oil molecules continue to diffuse out until the gel layer hardens with high wax content. Figure 2.1 shows a schematic of the aging process caused by the temperature difference across the deposit.

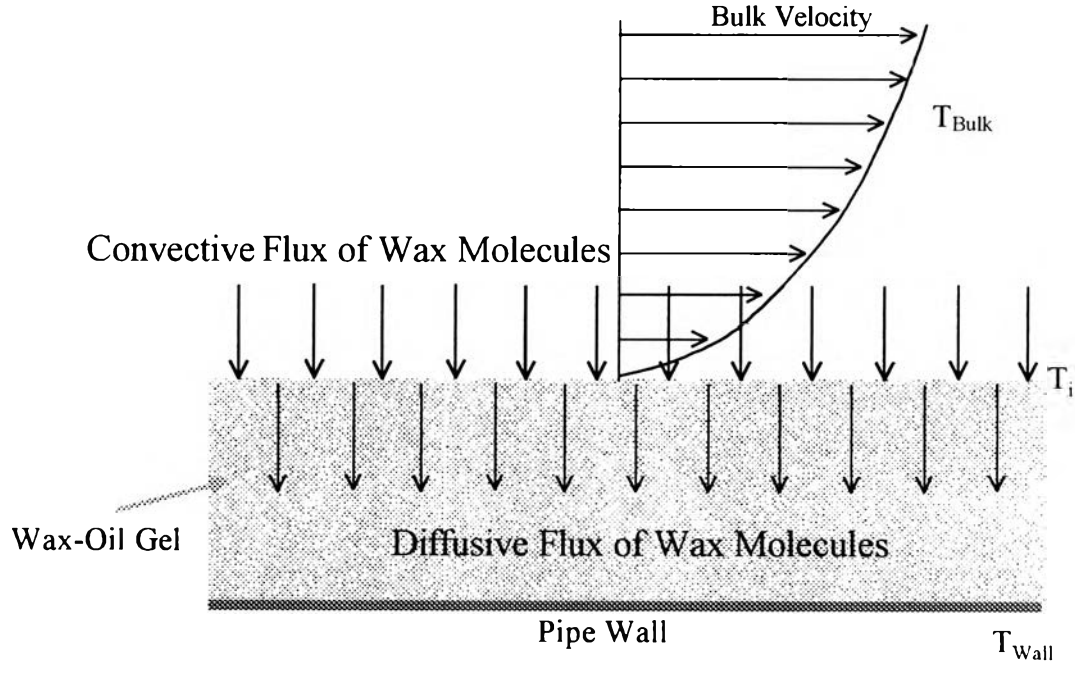

Figure 2.1 A schematic of the wax-oil deposition on the pipe-wall

2.3.2.2 Mechanical Force

The surface of the deposited gel is rough in nature. Hence, it is expected that the fluid flow over the gel surface will not only exert a shear force but also a compressive force on the gel deposit (Figure 2.2). This compressive force is expected to squeeze the oil out of the gel deposit and make it harder with time. However, the aging process of the gel deposit is a much weaker function of the compressive force exerted by flowing fluid on

the gels as compared to the temperature difference across the deposit (Singh *et al.*, 1999b). Thus, the prime cause of aging process is the temperature gradient across the gel deposit which leads to the counter diffusion of the wax and oil molecules into and out of the gel deposit.

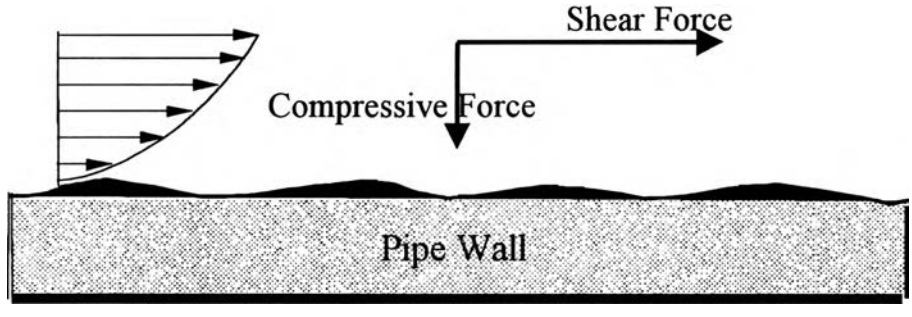

Figure 2.2 Forces on the gel deposit exerted by the flow of the wax-oil mixture

2.4 Thermodynamic Modelling

Several methods have been published concerning the prediction of wax formation in both crude oil and fuels. A large number of these models are, however, just empirical correlations relating wax appearance temperature (i.e. cloud point temperature) with fluid properties. A number of thermodynamic models have been proposed in the literature.

The first model developed by Won (1985) predicted solid-liquid equilibria of hydrocarbons using the ideal solution assumption. In a later paper, Won (1986) used a new modified regular solution theory for solid-liquid equilibria and SRK question of state for vapor-liquid equilibria. He used a modified solubility parameter in order to take the nonideality of solid solutions into account.

Hansen (1988) applied polymer solution theory for the oil (liquid) phase while the wax (solid) phase was assumed to be an ideal mixture. The

author used measured cloud points to determine the interaction parameters in their model, and the calculated and measured cloud points were therefore in reasonable agreement.

Coutinho *et al.* (1995) evaluated the activity coefficient models to describe the liquid phase nonideality for mixtures of alkanes. They concluded that the original Flory-Huggins model, regular solution theory, ideal solution theory, modified UNIFAC, and original Entropic free-volume model were not appropriate for the description of liquid phase in alkanes systems. The Flory free-volume and a modified version of Entropic free-volume were shown to be the simplest and the most reliable models.

A number of studies (Dorset, 1990; Snyder *et al.*, 1992; and Dirand *et al.*, 1998) showed that when binary normal alkane mixtures were cooled, the precipitation was unstable and segregated into two solid phases, provided the chain-length difference between the two alkanes exceeding a certain value. Hansen *et al.* (1991) observed phase transitions of the precipitated wax from North Sea crude oils. Dirand *et al.* (1998) performed the x-ray diffraction analyses for multicomponent paraffin wax. They observed the solid-solid transition of orthorhombic crystals.

Lira-Galeana *et al.* (1996), based on the above observations, developed a thermodynamic multi solid-wax model. In this model, each solid phase was described as a pure component which did not mix with other solid phases. The stability analysis was also used in the calculation for multi solid-liquid equilibria.

Pauly *et al.* (1998) stated that the solid solution model described by Wilson equation leaded to a satisfactory representation of narrow paraffin distribution. However, when paraffin distribution widened out, the nonideality of solutions increase and the model over-estimated the precipitation of the lightest components. To overcome this problem, assuming that the high nonideality between the heaviest and the lightest paraffins leaded to the

coexistence of several solid solutions, Coutinho (1998) proposed to use the UNIQUAC Model, which allows solid phase slits, instead of Wilson equation.

2.4.1 Solid - Liquid Equilibrium

The wax formation is treated as a solid–liquid equilibrium of paraffins between a liquid phase of solvent and an orthorhombic solid phase of paraffins. The solid–liquid equilibrium can be described by an equation relating the composition of component *i* in the solid and liquid phases with their non-ideality and the thermophysical properties of pure component.

The equilibrium condition is the equality of fugacities of each component in both phases:

$$f_i^S = f_i^L \tag{2.1}$$

Since no equation of state is available for solids, the equilibrium condition is alternatively expressed in terms of deviations to standard states as:

$$x_i \gamma_i^L f_i^{0,L} \exp\left(\int_{P_{ref}}^{P} \frac{v_i^L}{RT} dP \right) = s_i \gamma_i^S f_i^{0,S} \exp\left(\int_{P_{ref}}^{P} \frac{v_i^S}{RT} dP \right) \tag{2.2}$$

A thermodynamic cycle, outlined in the enthalpy-temperature diagram of Figure 2.3, is used to obtain a relation between the standard state fugacities as follows:

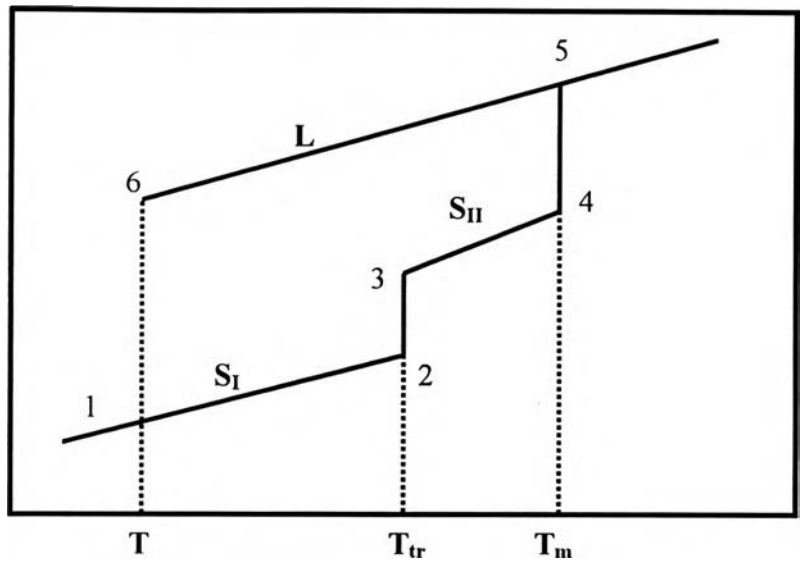

Figure 2.3 Enthalpy-temperature diagram for a solid/liquid equilibrium (Dauphin *et al.*, 1999)

The standard state is defined as the pure solid and pure subcooled liquid at temperature T at the saturation pressure. The temperatures T_m and T_{tr} are, respectively, the triple point temperatures of melting and of solid phase transition.

The change in Gibbs free energy for a component between the liquid and the solid phases can be related to the standard state fugacities by

$$\Delta g_{1\to6} = RT \ln \frac{f^{0,L}}{f^{0,S}} \tag{2.3}$$

The Gibbs free energy is also related to the enthalpy and entropy changes by

$$\Delta g_{1\to6} = \Delta h_{1\to6} - T \Delta s_{1\to6} \tag{2.4}$$

Both entropy and enthalpy are state functions and therefore independent of the path followed in the phase transition, thus neglecting the

effect of pressure differences between the actual pressure P and triple point pressures:

$$\underset{1\to6}{\Delta h} = \underset{1\to2}{\Delta h} + \underset{2\to3}{\Delta h} + \underset{3\to4}{\Delta h} + \underset{4\to5}{\Delta h} + \underset{5\to6}{\Delta h} \tag{2.5}$$

$$\underset{1\to6}{\Delta s} = \underset{1\to2}{\Delta s} + \underset{2\to3}{\Delta s} + \underset{3\to4}{\Delta s} + \underset{4\to5}{\Delta s} + \underset{5\to6}{\Delta s} \tag{2.6}$$

The variations of enthalpy in each step can be rewritten in terms of heat capacities, Cp, and enthalpies of phase transition

$$\underset{1\to6}{\Delta h} = \int_{T}^{Ttr} Cp_{S_I}\,dT + \Delta h_{tr} + \int_{Ttr}^{Tm} Cp_{S_{II}}\,dT + \Delta h_{m} + \int_{Tm}^{T} Cp_{L}\,dT \tag{2.7}$$

Similarly the entropy change can be written as:

$$\underset{1\to6}{\Delta s} = \int_{T}^{Ttr} \frac{Cp_{S_I}}{T}\,dT + \Delta s_{tr} + \int_{Ttr}^{Tm} \frac{Cp_{S_{II}}}{T}\,dT + \Delta s_{m} + \int_{T_m}^{T} \frac{Cp_{L}}{T}\,dT \tag{2.8}$$

At the phase transitions the entropy variations can be replaced by:

$$\Delta s_{tr} = \frac{\Delta h_{tr}}{T_{tr}} \tag{2.9}$$

and

$$\Delta s_{m} = \frac{\Delta h_{m}}{T_{m}} \tag{2.10}$$

Replacing Eqs. (2.7) and (2.8) in Eq. (2.4) and equating the latter with Eq. (2.3) there comes:

$$\ln\frac{f^{0,L}}{f^{0,S}} = \frac{\Delta h_{tr}}{RT_{tr}}\left(\frac{T_{tr}}{T}-1\right)+\frac{\Delta h_{m}}{RT_{m}}\left(\frac{T_{m}}{T}-1\right)+\frac{1}{RT}\left[\int_{T}^{Ttr} Cp_{S_I}\,dT+\int_{Ttr}^{Tm} Cp_{S_{II}}\,dT+\int_{T_m}^{T} Cp_{L}\,dT\right]$$
$$-\frac{1}{R}\left[\int_{T}^{Ttr} Cp_{S_I}\,dT+\int_{Ttr}^{Tm} Cp_{S_{II}}\,dT+\int_{T_m}^{T} Cp_{L}\,dT\right] \qquad (2.11)$$

From Eq. (2.2) an alternative expression for the ratios of standard states fugacities is obtained

$$\frac{f^{0,L}}{f^{0,S}} = \frac{s\gamma^{S}}{x\gamma^{L}}\exp\left(\int_{\Pr ef}^{P}\frac{v^{S}-v^{L}}{RT}dP\right) \qquad (2.12)$$

The substitution of Eq. (2.12) in Eq. (2.11) provides a general equation for solid/liquid equilibrium with identical results.

Some simplifying assumptions are commonly applied to the general equation of solid/liquid equilibrium. For hydrocarbon systems it will be assumed that:

- The temperature and enthalpy of phase transition at the triple point, and at the system pressure P are identical
- The ratio of standard state fugacities is temperature independent
- The heat capacities are temperature independent
- The heat capacities are identical in all solid phases
- The difference between the heat capacities of the liquid and solid phases is constant and can be properly described by the value at the melting point temperature (ΔCp_m)

The resulting equation of equilibrium is:

$$\ln \frac{s\gamma^{s}}{x\gamma^{L}} = \frac{\Delta h_m}{RT_m}\left(\frac{T_m}{T}-1\right)+\frac{\Delta h_{tr}}{RT_{tr}}\left(\frac{T_{tr}}{T}-1\right)-\frac{\Delta Cp_m}{R}\left(\frac{T_m}{T}-\ln\frac{T_m}{T}-1\right) \qquad (2.13)$$

This equation can be written for each of the n components present at the equilibrium.

$$\ln \frac{s\gamma^{s}}{x\gamma^{L}} = \frac{\Delta h_m}{RT_m}\left(\frac{T_m}{T}-1\right)+\frac{\Delta h_{tr}}{RT_{tr}}\left(\frac{T_{tr}}{T}-1\right) \qquad (2.14)$$

The heat capacity term and pressure term has been neglected for simplification.

2.4.2 Liquid Phase Non-ideality

The activity coefficient, in most activity coefficient models, can be expressed as the product of two contributions: a combinatorial part accounting for the differences in size and shape between the molecules and residual part due to energetic interactions between the components.

$$\gamma_i = \gamma_i^{comb}\gamma_i^{res} \qquad (2.15)$$

where γ_i is the activity coefficient of component i

An additional contribution owing to free-volume (fv) is needed for mixtures with components differing significantly in size.

$$\gamma_i = \gamma_i^{comb}\gamma_i^{fv}\gamma_i^{res} \qquad (2.16)$$

Hydrocarbon mixtures are a particular case of mixtures where one or more of these contributions can be ignored. They are known to behave almost athermally, meaning that the activity coefficient is almost temperature independent. In these cases, the residue contribution may be assumed to be

small and the deviations from ideality in the liquid phase are considered to arise from the shape and free-volume differences between the components.

In this work, the activity coefficient used for the liquid phase can be described by using Flory free-volume that use only a combinatorial-free-volume term without a residual contribution.

The combinatorial term for Flory free-volume can be expressed in the following general form

$$\ln \gamma_i^{comb} = \ln \frac{\phi_i}{x_i} + 1 - \frac{\phi_i}{x_i} \qquad (2.17)$$

where ϕ_i is the composition fraction of component *i* defined by

$$\phi_i = \frac{x_i \left(V_i^{1/3} - V_{wi}^{1/3}\right)^{3.3}}{\sum_j x_j \left(V_j^{1/3} - V_{wj}^{1/3}\right)^{3.3}} \qquad (2.18)$$

where V_i is the molar volume of component i (Elbro *et al.*, 1991)

V_{wi} is the van der Waals volume of component i

2.4.3 Solid Phase Non-ideality

In this study, the solid phase non-ideality was described by a well known local composition models, UNIQUAC which allows multi-solid phase equilibrium calculation. The UNIQUAC equation used in this work can be written as

$$\frac{g^E}{RT} = \sum_{i=1}^{n} s_i \ln\left(\frac{\Phi_i}{s_i}\right) + \frac{Z}{2}\sum_{i=1}^{n} q_i s_i \ln\frac{\theta_i}{\Phi_i} - \sum_{i=1}^{n} s_i q_i \ln\left[\sum_{j=1}^{n} \theta_j \exp\left(-\frac{\lambda_{ij}-\lambda_{ii}}{q_i RT}\right)\right] \qquad (2.19)$$

with

$$\Phi_i = \frac{x_i r_i}{\sum_{j=1}^{n} x_j r_j} \qquad (2.20)$$

and

$$\theta_i = \frac{x_i q_i}{\sum_{j=1}^{n} x_j q_j} \qquad (2.21)$$

and using structural parameters *r* and *q* estimated to take into account the specificity of the interactions in the solid phase:

$$r_i = 0.1483 \cdot r_{iorg} \qquad (2.22) \qquad \text{and} \qquad q_i = 0.1852 \cdot q_{iorg} \qquad (2.23)$$

For the description of the non-ideality of the orthorhombic solid phase of n-alkanes, the pair interaction energies between identical molecules are estimated by relating them to the enthalpy of sublimation of the orthorhombic crystalline phase of the pure component

$$\lambda_{ii} = -\frac{2}{Z}\left(\Delta h_{sblm_i} - RT\right) \qquad (2.24)$$

where Z is the coordination number and has a value of Z = 6 for the n-alkane orthorhombic crystals. Δh_{sblm} is the enthalpy of sublimation of the pure n-alkane.

The estimation of λ_{ij}, in this work, was based on the following hypothesis:

The energetic interactions between two molecules arise along the contact surface of these molecules. In the solid phase chain molecules act, to a large extent, as stiff rods. In this case the contact surface would be independent of the length of the long molecule as schematically shown in Figure 2.4. If this hypothesis is correct this would be the same as the interaction energy between two identical short molecules:

$$\lambda_{ij} = \lambda_{jj} \qquad (2.25)$$

where *i* and *j* represent the long and short n-alkane molecules, respectively. This hypothesis will be valid if the molecules are not very different in size otherwise the extremities of the long molecules will bend and further interactions between the molecules will arise eventually destroying the simplified picture described in Figure 2.4 and by Eq. (2.25). However, in the paraffinic solid phases, there would be mutually insoluble. Therefore, the

paraffinic solid phase will keep itself within the range of validity of the hypothesis.

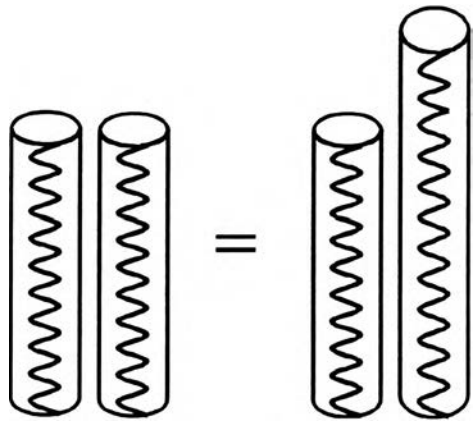

Figure 2.4 Axial contact surfaces between two identical and between two non-identical n-alkane molecules in the solid phase